

A.R. Stepanyuk, Y.A. Boychuk, T.N. Tsugorka,  
Y.I. Drebot, I.V. Lushnikova, T.A. Pivneva, P.V. Belan

## Estimating transmitter release rates and quantal amplitudes in central synapses from postsynaptic current fluctuations

*Декілька нових підходів, що були нещодавно введені для аналізу швидкості вивільнення нейромедіатора у центральних синапсах, хоча і дозволи поглибити наші знання про нервову передачу все ще залишили багато питань, які потребують розв'язання. У нашій роботі ми представляємо докази того, що новий метод, котрий був нещодавно розроблений Сакабою та Неером для дослідження нервової передачі у calyx of Held, гігантському глутаматергічному синапсі, може бути також застосований для оцінки швидкості вивільнення нейромедіатора та середніх амплітуд квантів струму малих центральних синапсах. За допомогою моделювання гальмівної синаптичної передачі у нейронах гіпокампа ми показали, що дефіцит просторової фіксації мембранного потенціалу, який може спостерігатися у синаптичних контактах, що розподілені по дендритному дереву, не є суттєвими для застосування нового методу у разі, коли синапси компактно розподілені або розташовані близько до соми нейрона і коли швидкість вивільнення нейромедіатора є нижчою ніж  $1 \text{ мс}^{-1}$ . У другому наборі симуляцій ми також довели, що при швидкостях вивільнення вказаних вище, десенситизація та насичення постсинаптичних ГАМК<sub>A</sub>-рецепторів не заважає точно оцінювати швидкість вивільнення нейромедіатора та середню амплітуду квантів. Таким чином, запропонований підхід, який базується на аналізі флуктуацій постсинаптичних струмів за умов стаціонарного або повільно змінного вивільнення нейромедіатора, може бути застосований для досліджень малих центральних синапсів.*

### INTRODUCTION

To understand mechanisms underlying pre- and postsynaptic modifications in the efficacy of synaptic connections taking place during asynchronous release and neurotransmitter spillover in many types of central synapses [1, 2, 3, 7, 8, 11, 12] one has to know (or at least estimate) a release rate and averaged amplitude of quantal events contributing to the postsynaptic currents. By the present moment this problem has not been satisfactory resolved. An interesting approach to estimate the above mentioned parameters has been recently suggested by Sakaba and Neher [15] and used by these authors to study some as-

pects of glutamatergic synaptic transmission in a giant synapse of rodent calyx of Held. It is suggested in the approach that an amplitude distribution of quantal events during prolonged synaptic activity is similar to a distribution of miniature postsynaptic currents. It has been possible to effectively voltage clamp both a postsynaptic neuron and presynaptic terminal doing this suggestion reasonable in the calyceal synapse. Unfortunately, it is hardly true in the most central synapses mainly due to a complex neuronal morphology. Dendritic filtration of synaptic currents and their interaction between themselves and voltage-dependent plasma membrane conductances can lead to substantial changes in the distri-

© A.R. Stepanyuk, Y.A. Boychuk, T.N. Tsugorka, Y.I. Drebot, I.V. Lushnikova, T.A. Pivneva, P.V. Belan

bution of quantal events in comparison with the mIPSC distribution possibly resulting in inapplicability of the method to the central synapses. Another problem with this method is related to desensitization and/or saturation of postsynaptic receptors by consecutive release of synaptic vesicles taking place in the same synapse during prolonged exocytosis. This can also lead to substantial changes in the distribution of quantal amplitude and errors in determining of a release rate function and averaged quantal amplitude.

In this work the applicability of the method in order to estimate release rates and averaged quantal amplitudes in small central synapses was tested by means of different simulation approaches.

## METHODS

**Tissue cultures.** Hippocampi from newborn rats were enzymatically dissociated with 0.05% pronase E [13]. Cell suspension at the initial density of  $3-5 \cdot 10^5$  cells per  $\text{cm}^2$  was plated on glass coverslips coated with laminine and poly-L-ornithine. The feeding solution consisted of minimal essential medium, 0.6% glucose, 1 mM glutamine, 26 mM  $\text{NaHCO}_3$ ,  $10 \mu\text{g} \cdot \text{ml}^{-1}$  insulin and 10% horse serum. All cultures were used for the experiments after 14 days plating (14–19 days in most of the experiments).

**Electrophysiological recordings.** Neurones growing in the cultures were visualized through a 40X objective on an inverted microscope (Axiovert, “Zeiss”, Germany). Whole-cell patch-clamp recordings were obtained from one or two neurones using EPC-7 (“List”, Germany) and RK-400 (“BioLogic”, France) amplifiers. In dual patch clamp experiments presynaptic neurons held at  $-60$  mV were stimulated at the frequency of 0.1–0.2 Hz or 20–60 Hz by 1–10 ms voltage steps to  $-10$  mV. In a part of experiments presynaptic neurons were extracellularly stimulated via a patch pipette placed in the vicinity of the presynaptic neurons’ soma using a stimulator isolator

(ISO-Flex, “A.M.P.I.”, Israel). The stimulation pipette was filled with an extracellular solution without glutamate blockers and glucose. Voltage pulses of 0.5–1 ms duration with amplitudes necessary to induce an action potential in presynaptic neurons (typically 20–40 V) were applied at the frequency of 0.1–0.2 Hz. Postsynaptic neurones were clamped at  $-60$  mV or at  $-0$  mV. All patch pipettes had a resistance of 3–5 M $\Omega$  when filled with an intracellular solution.

The intracellular solution contained (in mM): Cs gluconate – 100, CsCl – 30,  $\text{MgCl}_2$  – 4,  $\text{Na}_2\text{ATP}$  – 4, EGTA – 10, HEPES – 10; pH 7.3–7.4, 270–280 mOsm. Intracellular sodium channel blocker, QX-314, was added to the intracellular solution to improve a voltage clamp. We suggested that  $\text{Cs}^+$  and QX-314 also blocked most of plasma membrane voltage-operated conductances leaving  $\text{GABA}_A$  receptor channels the only substantial conductance in the postsynaptic neuron. The extracellular solution contained (in mM): NaCl – 140, KCl – 4,  $\text{CaCl}_2$  – 2,  $\text{MgCl}_2$  – 1, HEPES – 10, glucose – 10, DL-AP5 – 0.05, CNQX – 0.01; pH 7.3–7.4, 290–300 mOsm. With this combination of intra/extracellular solutions the reversal potential of  $\text{GABA}_A$ -receptor mediated currents was near  $-30$  mV. Miniature inhibitory postsynaptic currents (mIPSCs) were recorded in the presence of 1 mM of tetrodotoxin (TTX).

Glutamate receptor blockers were purchased from “Tocris” (UK); TTX and QX 314 – from “Alamone Lab” (Israel); all other chemicals were purchased from “Sigma” (Germany). All experiments were conducted at room temperature (20–22°C).

An access resistance 7–20 M $\Omega$  was compensated by 50–70%. An uncompensated access resistance (typically 5–7 M $\Omega$ ) was always less than 10 M $\Omega$  in all presented experiments. A current-voltage relationship was measured for each postsynaptic neuron and 100% off-line access resistance compensation was applied as proposed earlier [17]. Currents were low-pass filtered at 3 kHz and stored at 10 or 20 kHz.

**Noise Analysis.** In order to estimate possible values of release rates and average quantal sizes during the decay phases evoked IPSC we have adapted a method recently proposed by Neher and Sakaba [15] for studies of synaptic transmission at the Calyx of Held. Based on their results we have developed a modification of their method, which is applicable for studies of the synaptic transmission at GABAergic hippocampal synapses. The main addition to the previous method is a possibility to estimate faster changing release rates.

Briefly, the method is based on estimation of release rates or average quantal sizes from a noise of the records. Since the evoked current is composed of a set of unquantal events they, together with GABA<sub>A</sub> channels and equipment should contribute to the noise of the current. It is possible to show that under conditions when other sources of noise are removed (e.g. by a proper filtration) cumulants of the noise signal generated by a stream of randomly occurring quantal events are proportional to a release rate,  $\xi(t)$ , and to the integral over  $n^{\text{th}}$  power of quantal event time course. Using this approach which is based on Campbell's theorem Neher and Sakaba [15] showed that:

$$\xi = \frac{\lambda_2^3 I_3^2}{\lambda_3^2 I_2^3} \quad h = \frac{\lambda_3 I_2}{\lambda_2 I_3}$$

where  $\lambda_2, \lambda_3$  are variance and skew of filtered traces;  $I_2, I_3$  are notations for the integral over the 2<sup>nd</sup> and 3<sup>th</sup> power of the normalized filtered quantal event waveform.

The authors have also shown that these estimates are valid if the amplitude distribution of quantal events during the release is the same as mIPSC distribution or at least a value

$$H = \frac{\langle h^2 \rangle * \langle h \rangle}{\langle h^3 \rangle}$$

where  $\langle h \rangle, \langle h^2 \rangle,$  and  $\langle h^3 \rangle$  are expectation values for respective powers of quantal amplitude distribution, is preserved.

It was also shown that accuracy of this variance estimation is reversibly proportional

to square root of the number of independent samples that can be obtained during the observation interval. I.e. the longer observation interval the more accurate estimation of release rate can be obtained. In order to increase the accuracy in experiments we repeated a given protocol 40-100 times and averaged the variance in a given window over all traces.

A high pass filtering was implemented to eliminate low frequency trends and nonstationarities and to shorten the underlying unquantal events. The latter also permitted to decrease sampling time thereby increasing time resolution of the method. The filtering was performed by differentiation as described earlier by a customized routine written in Andatra software. The filter parameters were as follows:

A low pass filtering was also performed to suppress channel and instrumentation noise. Averaging sliding window of 0.8–2.0 ms was used for this purpose. This filtering was also performed in Andatra software.

To estimate a contribution of GABA<sub>A</sub> channel noise to the total variance we applied the same steps of high and low pass filtration (as we did for evoked IPSC) to a decay phase of miniature IPSC and to equal in time parts of the records preceding the mIPSC presumably having no channel activity. Then variances of these filtered records were calculated and averaged for all mIPSC and activity free traces, respectively, in a sliding window equal in size to a time window of low pass filter. No changes in variance during the decay of mIPSC were observed. We did not also observe any significant difference in variances during the decay of mIPSC and during activity free intervals of these filtered records. Thus we concluded that the channel noise did not contribute to the total variance of filtered mIPSC and, therefore, we disregard it when calculating quantal-induced variance of the IPSC.

We assumed that instrumentation noise and mIPSC-induced noise are statistically in-

dependent. Therefore, variance due to instrumentation noise could be subtracted from the total variance to leave quantal-induced variance during the decay of IPSC. In practice the mean variance calculated during 50 ms time window preceding the evoked IPSC was subtracted from the total variance during evoked IPSC decay.

**Deconvolution.** Assuming a linear summation of quanta during the evoked IPSC and independence of the quantal size and waveform on a moment of a quantal onset the release rate can be also determined using deconvolution [14, 16]. According to this method the mean evoked IPSC,  $\langle I(t) \rangle$ , is a convolution of mean quantal IPSC,  $\langle E(t) \rangle$ , and the release rate,  $\xi$ . I.e.

$$\langle I(t) \rangle = \int \xi(\tau) \langle E(t - \tau) \rangle d\tau$$

Thus, the release rate can be determined from the above equation. Deconvolution was performed numerically in Andatra software as a reversed Furrier transform of a ratio of the fast Fourier transforms of  $\langle I(t) \rangle$  and  $\langle E(t) \rangle$ .

**Simulations.** Monte Carlo simulations of evoked IPSC based on the release rates determined from Deconvolution were performed to verify the accuracy of release rate estimation obtained from noise analysis. Simulations performed in Andatra software created the evoked currents as a sum of quantal IPSCs according to a specified release rate as previously described [14]. A release process was considered as Poisson one during simulations. This suggestion seems reasonable since monosynaptic connections under study had 10-40 release sites (our own unpublished data), averaged number of ready release vesicles per site was about 10 [10], simulated release rates were in a range of  $0.05\text{--}2\text{ ms}^{-1}$  and a sample interval used for simulations was 0.05–0.1 ms. Thus, a probability for a given vesicle to be released was  $\ll 1$  implying Poisson process.

NEURON program [5, 6] was used to estimate if voltage clamp and space clamp (i.e. postsynaptic interaction of uniquantal cur-

rents) errors could contribute to the decay of evoked IPSC. Parameters of simulations were as follows:

1. Morphological parameters: a soma is a cylinder with a diameter  $15\mu\text{m}$  and length  $15\mu\text{m}$ ; a dendrite is a truncated cone with an initial diameter  $1.5\text{--}3.0\mu\text{m}$ , a diameter at the end  $0.5\mu\text{m}$  and length  $250\mu\text{m}$ .

2. Passive parameters: specific resistance of cytosol,  $R_i=200\text{ Om}\cdot\text{cm}$ ; membrane conductance,  $G_m=0.0001\text{ S}/\text{cm}^2$ , membrane potential,  $E=-65\text{ mV}$ .

3. GABAergic current at each synapse was considered as a product of two exponentials resulting in  $\tau_{\text{rise}}$  of 0.3 ms,  $\tau_{\text{decay}}$  of 20ms; averaged conductances 300 and 1200pS; mIPSC amplitude distribution was used to produce a respective conductance distribution; reversal potential,  $E=-35\text{ mV}$ .

4. Holding potential was chosen at  $-10\text{ mV}$ . Simulations were conducted for different access resistance and different distributions of synapses. A simulated access resistance was in a range 0.1–18.0 M $\text{Om}$ . Different distributions of 25 GABAergic synapses on the plasma membrane of neuronal soma and dendrite were simulated.

## RESULTS AND DISCUSSION

Time courses of prolonged (induced by tetanus) and single evoked inhibitory postsynaptic currents (pIPSCs and ePSCs) occurring in GABAergic synapses of hippocampal cultured neurons were recorded using a direct stimulation of a single presynaptic cells. Fig. 1 represents two examples of averaged prolonged and single stimulus IPSC. In these experiments a presynaptic neuron was either clamped in whole-cell configuration (Fig. 1,a) or stimulated extracellularly (Fig. 1,b) and postsynaptic currents recoded as indicated in the Methods. mIPSC were also recoded in the same postsynaptic neuron after collecting a substantial number of evoked IPSC by changing an extracellular solution to tetrodotoxin

(TTX)-containing one ( $1\mu\text{M}$  of TTX). A distribution of mIPSC amplitudes was used as a quantal amplitude distribution during prolonged IPSCs for the following deconvolution and noise analysis. Fig.1 shows that a decay of averaged prolonged IPSC is substantially slower than one of averaged single stimulus IPSC ( $P<0.001$ , unpaired t-test). This difference in decay kinetics represents an interesting phenomenon implicating that asynchronous (delayed) release of synaptic vesicles and/or nonlinear quantal interaction could occur af-

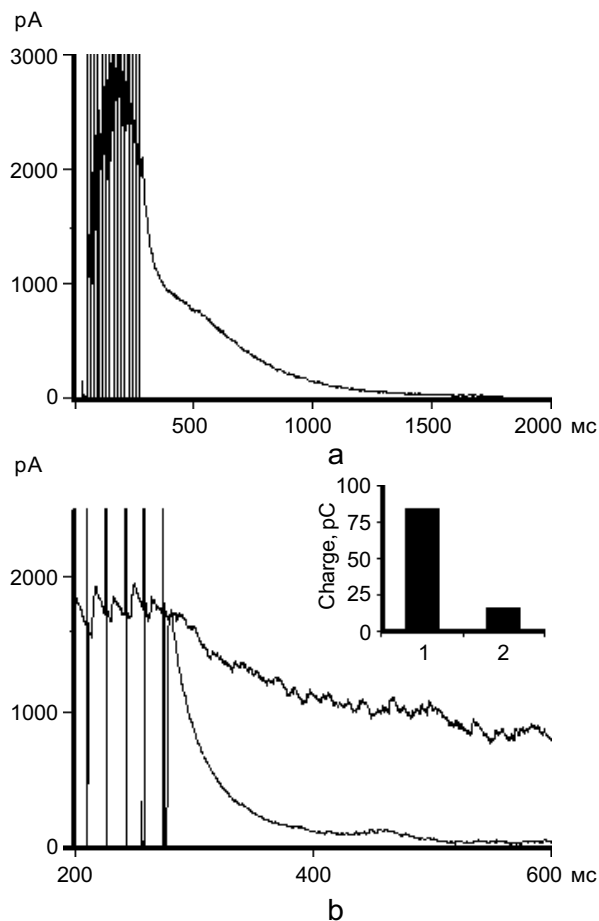


Fig. 1. Prolonged inhibitory postsynaptic currents occurring in GABAergic synapses of hippocampal cultured neurons:

a. An example of the prolonged IPSC after tetanic (15 stimuli, 60 Hz) stimulation of presynaptic neuron; b. Difference in decay kinetics of prolonged and single evoked IPSC. An insert shows a difference in charge transferred to soma per one action potential during the prolonged and single evoked IPSC

ter the tetanic stimulation of a particular synaptic connection between inhibitory presynaptic and postsynaptic neurons. This phenomenon may be important for both GABAergic synaptic transmission and proper neuronal functioning of the whole hippocampus since a charge transferred to the neuronal somata per one action potential can be dramatically increased when the frequency of presynaptic input is also increased. In a particular example illustrated in an insert of Fig. 1, b the charge per an action potential was increased almost 4 times when the frequency was changed from 0.3 to 60 Hz.

In order to show that a suggested by Sakaba and Neher approach can adequately estimate a release rate and averaged amplitude of quantal events we have suggested that mIPSC and quantal events during the decay of prolonged IPSC have the same amplitude distribution and that the quantal events are summed up linearly. Under these suggestions a release rate determined from deconvolution should be equal to one obtained by the above-mentioned approach and we directly tested it in order to show that the new approach works reliably.

A transmitter release rate was initially estimated from the experimental data presented in figure 1 by deconvolution of the averaged mIPSC from the averaged prolonged IPSC. Fig. 2, b demonstrates a time course of release rate determined by deconvolution. It shows that a substantial asynchronous release should occur to fully account for a prolonged decay of IPSC. After that Monte-Carlo simulations of prolonged IPSC based on a release rate obtained from deconvolution and mIPSCs amplitude distribution and their averaged waveform were performed as indicated in the Methods. Fig. 2, a demonstrates an averaged over 30 simulations prolonged IPSC together with an averaged experimental prolonged IPSC (30 experimental sweeps). It is clearly seen that the averaged traces coincide well indicating accuracy of the Monte-Carlo simulations. Application of the method suggested

by Sakaba and Neher to the simulated prolonged IPSC gave us a release rate function and averaged amplitude of quantal events equal to ones used in the simulations (Fig. 2,b). Thus, we concluded that the new approach can adequately estimate the release rate function and averaged amplitude of quantal events from postsynaptic current fluctuations at least

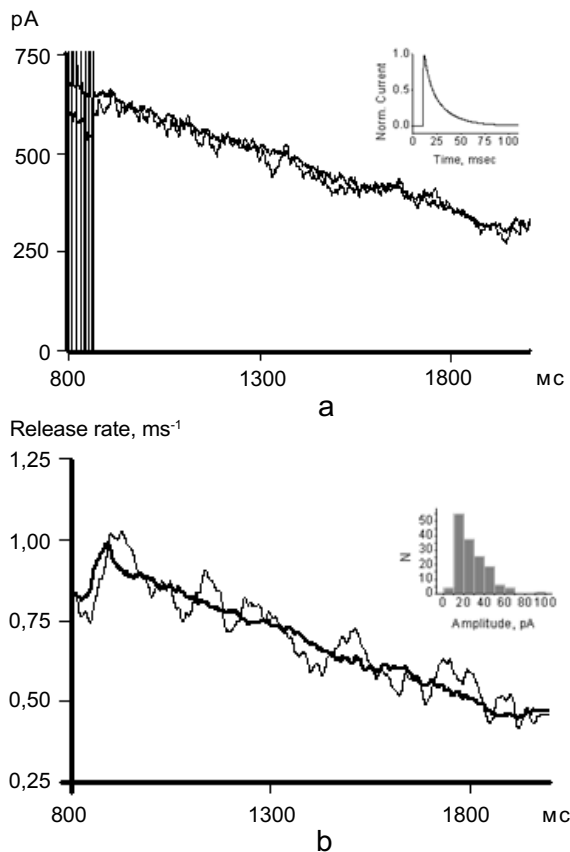


Fig. 2. Release rate estimations from the noise of prolonged IPSCs.

a, b. A release rate estimate from variance and skew of noise during prolonged IPSC. Initially the release rate was determined (thick trace in b) by deconvolving an averaged miniature IPSC (insert in a) from an averaged prolonged IPSC (thin trace in a). This release rate was used for Monte Carlo simulation of prolonged IPSC. A thick trace in a represents an averaged simulated prolonged IPSC. For simulations (20 traces), mIPSC amplitudes were randomly chosen from an amplitude distribution of experimentally recorded mIPSC (insert in a). A waveform of averaged miniature IPSC (insert in a) was used for the simulations. A release rate (thin line in b) was estimated afterwards from variance and skew of noise of simulated traces as indicated in METHODS

in simple experimental situations.

It is reasonable to suggest that at relatively low release rates (about 0.1–0.3 ms<sup>-1</sup>) it can be possible to directly count release events since they are not substantially overlapped. Thus, we have estimated and compared release rates in tails of the experimental prolonged currents (when the release rates are low) obtained by direct counting of the quanta and by the noise analysis of Sakaba and Neher.

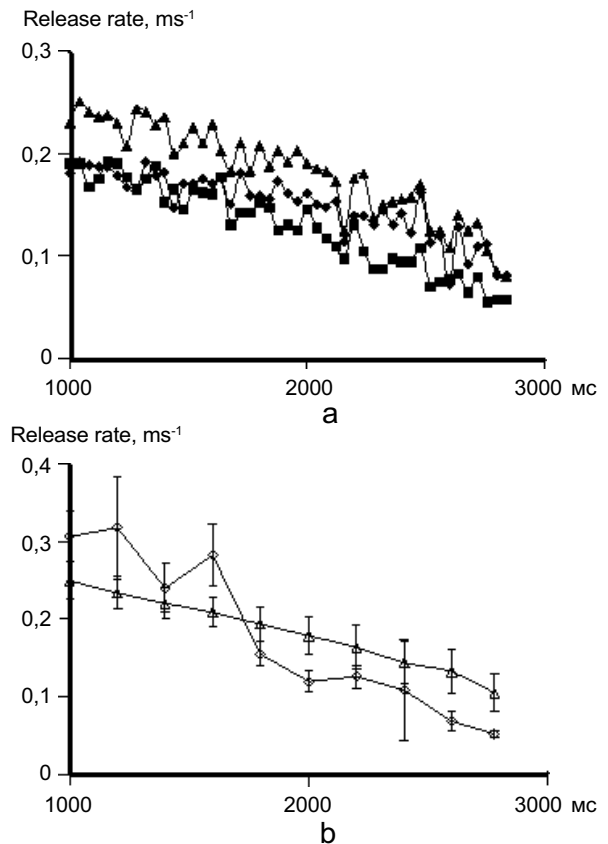


Fig. 3. Comparison of release rate estimates by noise analysis and direct counting of quanta.

a. Examples of release rate estimates by direct quantal counting. Traces represent a release rate obtained by direct counting of the quanta after wavelet denoising of original prolonged currents by customized algorithm (with a window of 5 ms and 10 pA, squares, and 1 ms, 7 pA, triangles). Circles represent the release rate estimate by counting peaks on variance of prolonged IPSC calculated after denoising and differentiation of original records. b. Release rates estimated by noise analysis (diamonds) and direct counting by the customized algorithm with a window of 1 ms, 7 pA (triangles)

The direct counting was employed after either initial wavelet denoising of original prolonged currents by customized algorithm or by counting peaks on variance of prolonged IPSC calculated after smoothing and differentiation of original records (Fig.3). The release rates estimated by both the direct counting and noise analysis were similar indicating that the suggested method works well at least at low release rates up to  $0.2\text{--}0.3\text{ ms}^{-1}$ .

In the next part of our work we performed simulation analysis of synaptic interaction influence on estimations of mean quantal amplitudes and release rates obtained by the new method. For that Monte Carlo simulations of prolonged IPSCs (using a release rate function obtained as in Fig.2 and mIPSC amplitude distribution) were carried out in NEURON environment with a two-compartment model of a neuron and different synaptic distributions over neuronal membrane. Morphology with a conic dendrite and cylindrical somata was used for the simulations (see Methods). 25 synapses were distributed over the plasma membrane of the simulated neuron as indicated in Fig. 4,c by circles. Fig. 4 demonstrates that there is a substantial intersynaptic interaction due to a problem with space voltage-clamp leading to a decrease of the current contributed by distal synapses. It results in a decrease of an integral current recorded by a patch pipette (Fig. 4,a), a change in its waveform (Fig. 4,b), and consequently in changes of a waveform and amplitude distribution of quantal events in comparison with mIPSCs. Fig. 5,a shows that intersynaptic interaction can result in many fold difference between averaged mIPSCs ( $h_0$ ) and averaged quantal events ( $h$ ) during a continues release that takes place during prolonged IPSCs. Of course, it can lead to a substantial error in estimating of release rates by the new method based on an assumption that the distribution of quantal events should be similar to mIPSC distribution. Therefore, the new approach was applied to the simulated IPSCs and averaged

amplitude of quantal events estimated by this approach ( $h_{\text{noise}}$ ) was compared with one calculated directly in NEURON environment. Fig. 5,b represents a ratio of  $h/h_{\text{noise}}$ . Comparison of traces drawn in diamonds in Fig. 5,a and b clearly shows that the new approach substantially improves an estimation of the

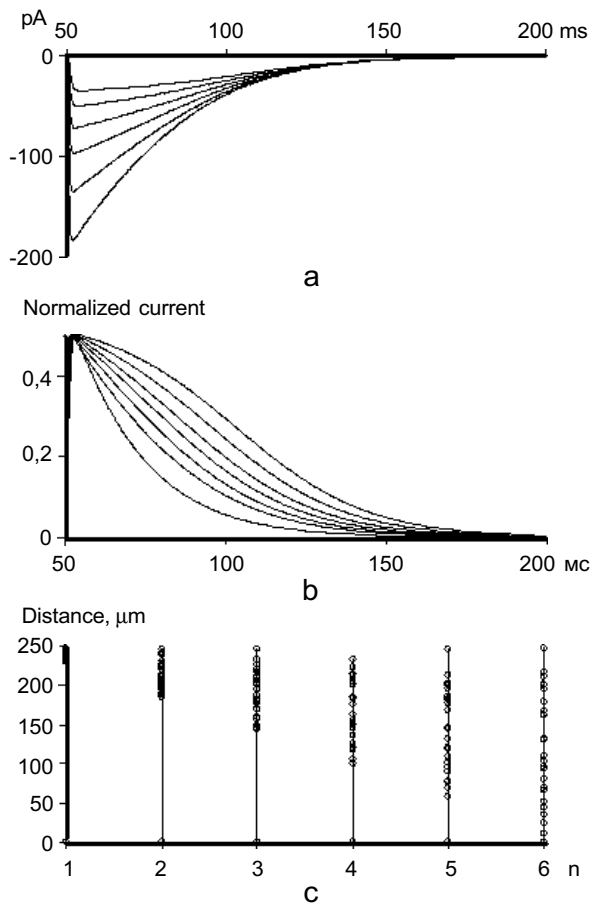


Fig. 4. Simulation of synaptic interaction influence on evoked IPSC amplitudes and waveforms.

a. An example of NEURON simulations of evoked IPSC. Two-compartment model with a cylindrical soma, conic dendrite and synaptic distributions as indicated in c was used. Morphology with a conic ( $1.5\text{--}0.5\text{ }\mu\text{m}$ ) dendrite of  $250\text{ }\mu\text{m}$  was simulated in this particular example. Experimental distribution of mIPSC amplitudes was used to produce a synaptic conductance distribution used in simulations. b. Normalized traces from a. c. Synaptic distributions used in the simulation experiments. 25 synapses with an averaged synaptic conductance of  $1200\text{ pS}$  were randomly distributed over different parts of dendrite as indicated in c by circles

averaged quantal amplitude (and hence the release rate function) in comparison with  $h_0$  for the case when synapses are co-localized on the neuronal dendritic tree. In spite of substantial (more than 2 times) reduction in the

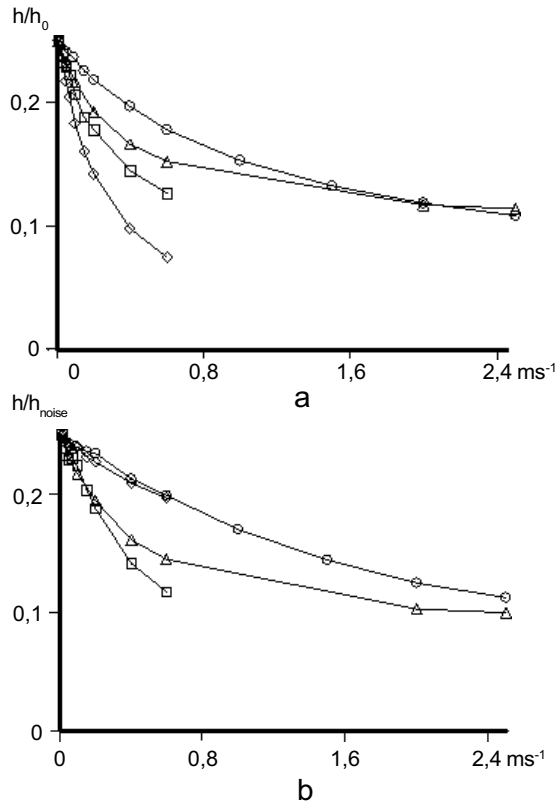


Fig. 5. Simulation analysis of synaptic interaction influence on estimations of averaged quantal amplitudes and release rates.

a. Changes in the mean quantal amplitude due to synaptic quantal interaction.  $h_0$  – the mean mIPSC amplitude;  $h$  – the mean quantal amplitude during steady-state release. Squares indicate changes in  $h/h_0$  ratio with changes in release rates for a dendritic synaptic distribution with 5 synapses on the soma and 20 synapses on 20 distal mm of a truncated conic (3.0 - 0.5  $\mu\text{m}$ ) dendrite of 250  $\mu\text{m}$  length; diamonds show a release rate dependence of  $h/h_0$  ratio for a distribution when all 25 synapses are randomly distributed over distal 25  $\mu\text{m}$  of the same conic dendrite; circles – the same synaptic distribution as for squares but synapses have a averaged synaptic conductance of 300 pS; triangles – all conditions as for circles but a shape of a dendrite is a truncated cone (1.5  $\rightarrow$  0.5  $\mu\text{m}$ ). b. A release rate dependence of a ratio of the averaged quantal amplitude,  $h$ , and the averaged quantal amplitude estimated from noise analysis,  $h_{\text{noise}}$ . Neuronal morphology and synaptic distributions are as indicated in a

averaged quantal amplitude the release rates and averaged quantal amplitudes could be estimated with a reasonable accuracy of 20% for release rates up to 0.8  $\text{ms}^{-1}$ . The same conclusion can be also obtained (simulations not shown) in a case of clustered synaptic distribution on different dendritic branches; the synaptic clusters have to be on approximately similar electrotonic distances from a neuronal soma. Thus, the new approach might be applicable to both proximal and distal compact synaptic distributions in order to estimate quantal amplitudes and release rates with accuracy of about 20% in a wide range of neuronal morphologies when the release rate is below 1  $\text{ms}^{-1}$ . Since compact synaptic distributions are widely represented in the central nervous system (e.g. synapses established by Shaffer collaterals on CA1 neurons) the approach might be of advantage in studies neurotransmission in such synapses. At the same time it is clear that if synapses are formed in electrotonically different neuronal compartments the approach is becoming quite inaccurate (squares in Fig. 5,a,b).

In the simulations described above a relatively high value of synaptic conductance was used. Decreasing the conductance led to substantial reduction in synaptic conductance interaction (circles in Fig. 5,a,b) and applicability of the proposed approach to studies of sparsely (but relatively proximally – up to 200  $\mu\text{m}$ ) distributed synapses at release rates up to 0.8  $\text{ms}^{-1}$  and with accuracy of about 20%. Although we have to confess that decreasing an initial dendritic diameter from 3.0 to 1.5  $\mu\text{m}$  once again resulted to inaccuracy in release rate estimations (triangles in Fig. 5,a,b). Therefore, morphological tracing of dendritic tree and localization of synapses on its branches by different modern techniques might be necessary in order to obtain accurate estimations of release rates in small central synapses.

Another problem, which can limit applicability of the method, is changes in distribution of quantal amplitudes in comparison with

mIPSC distribution originated from desensitization and/or saturation of postsynaptic receptors by preceding acts of quantal release. To test how these factors can influence estimating of release rates and averaged quantal amplitudes Monte Carlo simulations of GABA<sub>A</sub> receptor-mediated currents in a single GABAergic synapse were carried out. For these simulations we have considered that during prolonged inhibitory postsynaptic current each synapse spontaneously releases synaptic quanta with a probability for a quantum to be released in a time window  $\Delta t$  equal to  $x(t) \cdot \Delta t$  (where  $x(t)$  is a single synapse release rate function). A maximal value of a single synapse release rate estimated from experimental data (Fig. 1, 2) was used for Monte Carlo simulations. This value of release rate was calculated by dividing maximal release rates estimated from noise in the upper part (50 ms) of prolonged IPSCs by the number of synapses in a given monosynaptic connection. The former was estimated by means of the new approach whereas the later from a mean-variance analysis [4]. A simple binominal model of synaptic transmission was used in the mean-variance analysis. An averaged mIPSC amplitude obtained from postsynaptic recordings (Fig. 1) was used in the simulations. In an example given in figure 6 the release rate was set at  $0.03 \text{ ms}^{-1}$ . It was considered in the simulations that a quantal release produced a GABA concentration transient in a synaptic cleft with an instantaneous rising phase and monoexponential decay of 0.3 ms. A previously published kinetic scheme of GABA<sub>A</sub> receptor [9] was used in simulations. Some rate constants and GABA transient amplitude were changed to be in agreement with an experimental averaged mIPSC time course. The value of the constants were in  $\text{ms}^{-1} K_f$ , 0.003  $\text{mM}^{-1}$ ;  $k_b$ , 0.150;  $d_1$ , 0.013;  $r_1$ , 0.00013;  $d_2$ , 0.750;  $r_2$ , 0.015;  $c_1$ , 1.111;  $o_1$ , 0.200;  $c_2$ , 0.142;  $o_2$ , 2.500.

Fig. 6,a demonstrates an example of simulated current. It is clearly seen from the fig-

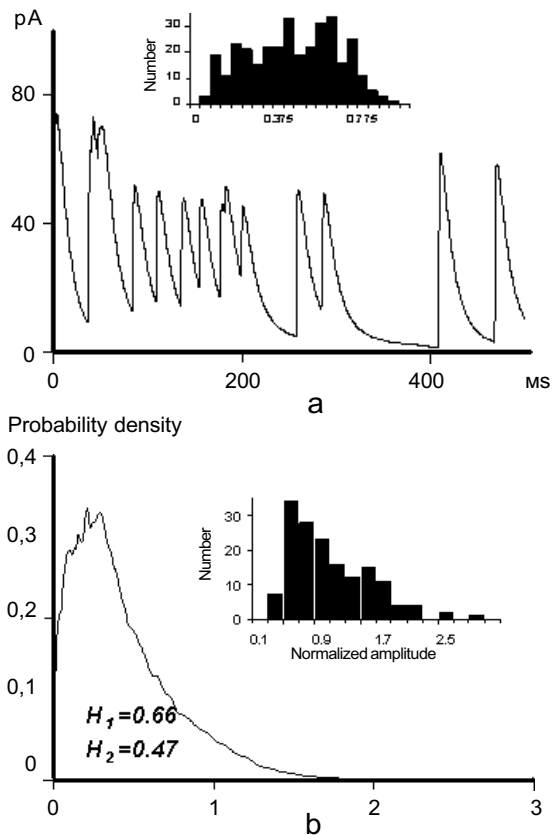


Fig. 6. Simulation analysis of desensitization/saturation influence on estimations of averaged quantal amplitudes and release rates.

a. Monte Carlo simulations of GABA<sub>A</sub> receptor-induced currents in a single synapse. Single synapse release rates were estimated from noise and mean-variance analysis. In a given example a single synapse release rate was set at  $0.03 \text{ ms}^{-1}$ . A previously published kinetic scheme of GABA<sub>A</sub> receptor fitted on the basis of our experimental results was used for simulations of GABA<sub>A</sub>R-mediated currents. For that some rate constants were changed to meet experimental mIPSC waveform and maximal open state probability. The value of the constants were in  $\text{ms}^{-1} K_f$ , 0.003  $\mu\text{M}^{-1}$ ;  $k_b$ , 0.150;  $d_1$ , 0.013;  $r_1$ , 0.00013;  $d_2$ , 0.750;  $r_2$ , 0.015;  $c_1$ , 1.111;  $o_1$ , 0.200;  $c_2$ , 0.142;  $o_2$ , 2.500. Synaptic GABA transient was fitted by sum of 2 exponentials. Changes in amplitude distribution originated in a single synapse due to desensitization/saturation are depicted in the insert. b. Changes in quantal amplitude distribution due to desensitization/saturation. Modified by desensitization/saturation amplitude distribution was obtained by convolution of original mIPSC amplitude distribution and a function shown in an insert in a. An insert represents an original mIPSC amplitude distribution

ure that the amplitudes of postsynaptic currents are substantially reduced due to desensitization and saturation of GABA<sub>A</sub> receptors. This reduction leads to dramatic changes in an amplitude distribution of postsynaptic currents generated in a single synapse (Fig. 6,a; insert). Changes in an amplitude distribution of a whole set of synapses of a given monosynaptic connection is presented in Fig. 6,b. An insert shows experimentally recorded mIPSC amplitude distribution of a given synaptic connection (the same as in Fig. 1) and a main graph demonstrates its transformation due to the receptor desensitization and saturation. The transformation was accomplished by convolution of original mIPSC amplitude distribution and a function shown in an insert in Fig.6,a. Despite a considerable shift to lower amplitude values due to the desensitization and saturation, a shape of the quantal amplitude distribution was reasonably preserved. As a result there was not a substantial change in H (Fig. 6,b), which constant value is a prerequisite of applicability of the new approach. Thus, only a minor error of 20% was introduced in estimating the averaged quantal value and consequently in estimating of release rates. Since this error was predicted for release rates close to maximal ones observed in our experiments than it should be reasonably small in the most part of tails of prolonged IPSCs.

Thus, as a result of simulations described above we have shown that the new approach suggested for studying release rates in compact central synapses (where a space voltage clamp is not an issue) may be successfully applied to examine synaptic transmission taking place in small central synapses. In GABAergic synapses of cultured hippocampal neurons having up to 30-40 separate release sites and distributed over a dendritic tree of postsynaptic neuron a slowly changing release rates up to 1 ms<sup>-1</sup> and an averaged amplitude of underlying quantal events could be faithfully estimated in certain experimen-

tal situations with an accuracy of 20%. We conclude that the new approach may be applied to study central synapses with moderate values of release rates in case of somatic and proximal dendritic innervation.

### Acknowledgements

*This work was supported by the Wellcome Trust grant to P.B.*

**A.R. Stepanyuk, Y.A. Boychuk, T.N. Tsugorka, Y.I. Drebot, I.V. Lushnikova, T.A. Pivneva, P.V. Belan**

### ESTIMATING TRANSMITTER RELEASE RATES AND QUANTAL AMPLITUDES IN CENTRAL SYNAPSES FROM POSTSYNAPTIC CURRENT FLUCTUATIONS

Several approaches recently introduced to analyze release rates in central synapses advanced our understanding of synaptic neurotransmission, however, leaving many questions still unresolved. In this work we present evidence that a new method recently developed by Sakaba and Neher to study neurotransmission in calyx of Held, a giant glutamatergic synapse, could be also applied for estimating release rate functions and averaged quantal sizes in small central synapses. By means of different simulation approaches applied to reproduce GABAergic neurotransmission in the hippocampus we have shown that possible problems with a spatial voltage clamp which can occur in synaptic connections distributed over a large area of dendritic tree are not crucial for applicability of the method when synapses are compactly distributed or located proximally and when release rates are below 1 ms<sup>-1</sup>. In another set of simulations we have also shown that at above mentioned release rates desensitization and/or saturation of postsynaptic GABA<sub>A</sub> receptors does not prevent accurate estimates of release rate and averaged quantal size. Thus, we conclude that the new approach based on analysis of fluctuations of postsynaptic currents under conditions of stationary release or moderately nonstationary conditions might be applicable to studies of small central synapses.

*A. A. Bogomoletz Institute of Physiology, National Academy of Sciences of Ukraine, Kiev*

### REFERENCES

1. Atluri P.P., Regehr W.G. Delayed release of neurotransmitter from cerebellar granule cells // *J. Neurosci* – 1998. – **18**. – P.8214–8227.
2. Auger C., Marty A. Heterogeneity of functional synaptic parameters among single release sites // *Neuron*. – 1997. – **19**. – P.139–150.

3. Brenowitz S., Trussell L.O. Minimizing synaptic depression by control of release probability // *J. Neurosci* – 2001. – **21**. – P.1857–1867.
4. Clements J.D., Silver R.A. Unveiling synaptic plasticity: a new graphical and analytical approach // *Trends Neurosci.* – 2000. – **23**, – P.105–113.
5. Hines M.L., Carnevale N.T. The NEURON simulation environment // *Neural Comput.* – 1997. – **9**. – P.1179–1209.
6. Hines M.L., Carnevale N.T. NEURON: a tool for neuroscientists // *Neuroscientist.* – 2001. – **7**. – P.123–135.
7. Jensen K., Jensen M.S., Bonefeld B.E., Lambert J.D. Developmental increase in asynchronous GABA release in cultured hippocampal neurons // *Neuroscience.* – 2000. – **101**. – P.581–588.
8. Jensen K., Lambert J.D., Jensen M.S. Tetanus-induced asynchronous GABA release in cultured hippocampal neurons // *Brain Res.* – 2000. – **880**. – P.198–201.
9. Jones M.V., Westbrook, G.L. The impact of receptor desensitization on fast synaptic transmission // *Trends Neurosci.* – 1996. – **19**. – P.96–101.
10. Kirischuk S., Grantyn R. A readily releasable pool of single inhibitory boutons in culture // *Neuroreport.* – 2000. – **11**. – P.3709–3713.
11. Kullmann D.M. Spillover and synaptic cross talk mediated by glutamate and GABA in the mammalian brain // *Prog Brain Res JID.* – 0376441. – 2000. – **125**. – P.339–351.
12. Lozovaya N.A., Kopanitsa M.V., Boychuk Y.A., Krishtal O.A. Enhancement of glutamate release uncovers spillover-mediated transmission by N-methyl-D-aspartate receptors in the rat hippocampus // *Neuroscience.* – 1999. – **91**. – P.1321–1330.
13. Melnick I.V., Chvanov M.A., Belan P.V. Rat hippocampal neurons maintain their own GABAergic synaptic transmission in culture // *Neurosci. Lett.* – 1999. – **262**. – P.151–154.
14. Neher E., Sakaba T. Combining deconvolution and noise analysis for the estimation of transmitter release rates at the calyx of held // *J Neurosci.* – 2001. – **21**. – P.444–461.
15. Neher E., Sakaba T. Estimating transmitter release rates from postsynaptic current fluctuations // *J. Neurosci JID.* – 8102140. – 2001. – **21**. – P.9638–9654.
16. Segal J.R., Ceccarelli B., Fesce R., Hurlbut W.P. Miniature endplate potential frequency and amplitude determined by an extension of Campbell's theorem // *Biophys J JID.* – 0370626. – 1985. – **47**. – P.183–202.
17. Traynelis S.F. Software-based correction of single compartment series resistance errors // *J Neurosci Methods.* – 1998. – **86**. – P.25–34.

*A. A. Bogomoletz Institute of Physiology, National Academy of Sciences of Ukraine, Kiev*

*Received 27.05.2004*